

CrossMark
click for updatesCite this: *Chem. Sci.*, 2015, 6, 1212

Bioorthogonal prodrug activation driven by a strain-promoted 1,3-dipolar cycloaddition†

Siddharth S. Matikonda,‡ Douglas L. Orsi,‡ Verena Staudacher,‡ Imogen A. Jenkins, Franziska Fiedler, Jiayi Chen and Allan B. Gamble*

Due to the formation of hydrolysis-susceptible adducts, the 1,3-dipolar cycloaddition between an azide and strained *trans*-cyclooctene (TCO) has been disregarded in the field of bioorthogonal chemistry. We report a method which uses the instability of the adducts to our advantage in a prodrug activation strategy. The reaction of *trans*-cyclooctenol (TCO-OH) with a model prodrug resulted in a rapid 1,3-dipolar cycloaddition with second-order rates of $0.017\text{ M}^{-1}\text{ s}^{-1}$ and $0.027\text{ M}^{-1}\text{ s}^{-1}$ for the equatorial and axial isomers, respectively, resulting in release of the active compound. ^1H NMR studies showed that activation proceeded *via* a triazoline and imine, both of which are rapidly hydrolyzed to release the model drug. Cytotoxicity of a doxorubicin prodrug was restored *in vitro* upon activation with TCO-OH, while with *cis*-cyclooctenol (CCO-OH) no activation was observed. The data also demonstrates the potential of this reaction in organic synthesis as a mild orthogonal protecting group strategy for amino and hydroxyl groups.

Received 24th August 2014
Accepted 7th November 2014

DOI: 10.1039/c4sc02574a

www.rsc.org/chemicalscience

The ability to deliver drugs only at their site of action is highly advantageous in cancer therapy. Unfortunately, the current arsenal of drugs used to treat cancer are generally non-selective, leading to toxic side effects.^{1–3} To combat toxicity, prodrug activation strategies have been developed.^{3–5} Activation, *via* cleavage of a deactivating linker on the prodrug, is usually triggered by an overexpressed enzyme or change in the tumor environment (e.g. pH). However, the changes are often so subtle that selective activation of small molecule prodrugs is low, with many linkers susceptible to non-specific, off-target hydrolysis.³

Antibody–drug conjugates (ADCs) have the potential to avoid some of the problems associated with small molecule prodrugs and have been utilised effectively over the past few decades.⁶ However, there are still some inherent problems with ADCs including; (1) immunogenicity of the antibody, (2) difficulty in maintaining the balance between stability *vs.* cleavability of the antibody–drug linker, and (3) decreased potency of the drug as the effective concentration is limited by the number of cell surface receptors ($\sim 10^5$ receptors per cell) and number of molecules that can be attached to the antibody. In addition, low target-to-background drug ratios of monoclonal antibodies typically result in low tumor concentrations of the therapeutic agent.^{7,8} Pre-targeting strategies in which a non-toxic conjugate is allowed to accumulate at the tumor before administration of

the prodrug, e.g. antibody-directed enzyme prodrug therapy (ADEPT)^{9,10} and bioorthogonal chemistry,^{11–14} could help overcome the low tumor-to-background ratios as well as avoid the requirement of a cleavable (and potentially unstable) linker in the administered prodrug. While ADEPT has shown promise in cancer therapy, anti-enzyme immune responses have hindered its *in vivo* application.¹⁰

Over the past decade, bioorthogonal chemistry has found widespread utility in biological imaging.¹⁵ To date, however, there are only a handful of examples using bioorthogonal chemistry for *in vitro* prodrug activation strategies.^{11,16–20} The best examples using click chemistry are those of Robillard who utilized the Staudinger reaction,¹⁷ and more recently, the *trans*-cyclooctene (TCO)/tetrazine ligation for prodrug-activation.¹¹ The fast kinetics of the tetrazine ligation provide *in vivo* potential, however, this is yet to be demonstrated for prodrug activation and we envisage a number of challenges that could be encountered in future studies. These may include; (1) reduced reactivity of the TCO-conjugate when it is present in a sterically demanding environment (e.g. attached to both the antibody and cytotoxic drug), and (2) a low tumor-to-background ADC ratio leading to off-target release of the cytotoxic drug. Attachment of the tetrazine to the antibody would allow for pre-targeting with a non-toxic conjugate, however, the doxorubicin–TCO prodrug which would then need to be administered separately will be exposed to potential isomerization back to the unreactive *cis*-cyclooctene (CCO), a problem which is avoided when the TCO is attached to the antibody *via* a suitably designed linker.²¹

Inspired by the initial bioorthogonal activation strategies and the *in vivo* challenges that they posed, we set out to develop

School of Pharmacy, University of Otago, Dunedin, 9054, New Zealand. E-mail: allan.gamble@otago.ac.nz

† Electronic supplementary information (ESI) available. See DOI: 10.1039/c4sc02574a

‡ These authors contributed equally to the work.



a new bioorthogonal prodrug activation based on a 1,3-dipolar click reaction between a TCO and an azide. Interestingly, this click reaction has received much less attention than the strain-promoted 1,3-dipolar cycloaddition of cyclooctynes and azides (SPAAC) due to the instability of the formed adducts in aqueous conditions.^{15a,15c,22,23} In 1992, Shea reported a reaction between a strained TCO **2** and 2,4,6-trinitrophenylazide **1** in CDCl₃.²⁴ Triazoline **3** formed from this highly electron-deficient system could not be isolated. Instead a rearrangement in which diatomic nitrogen was released gave three isolated products; aldimine **4**, ketimine **5** and aziridine **6** (Scheme 1).

We recognized that analogues of imine **4** or **5**, when correctly attached to an electron-deficient self-eliminating linker (*e.g.* *p*-aminobenzoyloxycarbonyl, PABC),^{5,25} could have potential in targeted prodrug activation strategies (Fig. 1) or orthogonal protection/deprotection chemistry. If an imine could be generated *in situ* by a 1,3-dipolar cycloaddition (step 1–3), acid-catalyzed hydrolysis²⁶ in the tumor microenvironment (pH = 6.0–7.4)^{27,28} would lead to a rapid 1,6-elimination and removal of the PABC protecting group from the prodrug to release the active drug (step 4 and 5).^{25,26} While simple aryl azides can form stable triazolines in organic solvents,²⁹ we hypothesized that, in an aqueous environment, the reaction of a TCO and an aryl azide bearing an electron-deficient PABC group would favour *in situ* triazoline rearrangement *via* alkyl migration towards the desired imine rather than aziridine formation.²⁴

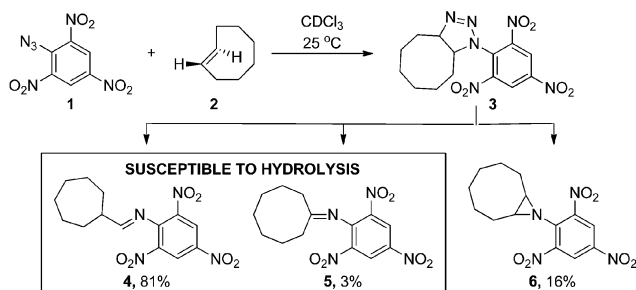
Herein we report the first *in vitro* example of a bioorthogonal prodrug activation strategy utilizing the 1,3-dipolar cycloaddition of an azide and a strained *trans*-cyclooctenol (TCO-OH). Our strategy demonstrates greater potential for bioorthogonally activated azide prodrugs *in vivo* as it holds two key advantages over the use of the Staudinger reaction for prodrug activation;¹⁷ (1) activation is 1–2 orders of magnitude faster with potential for future improvements (not possible with the Staudinger reaction),³⁰ and (2) TCO can be modified so that it is more metabolically stable (*i.e.* no deactivation by isomerization to the *cis*-isomer)²¹ than the oxidation prone and serum reactive phosphine.³⁰ Our results also demonstrate the potential use of the cycloaddition in synthetic chemistry as an orthogonal protection/deprotection strategy of –NH₂ and –OH functional groups.

In order for our strategy to succeed we first needed to determine if the labile aldimine was favored over the stable aziridine, therefore enabling release of the active drug. For

these proof-of-concept experiments two azido-PABC analogues were synthesized (Scheme 2). Coumarin probes **8a** and **8b**, masking a 7-hydroxycoumarin and 7-amino-4-methylcoumarin, respectively, were selected to investigate the mechanism and rate of the 1,3-dipolar cycloaddition, triazoline/imine degradation, and overall release of the drug from a carbonate and carbamate linked drug. The previously reported doxorubicin prodrug **9** was synthesized¹⁷ to examine *in vitro* bioorthogonal activation, and stability/activation of the aryl azide linker in mouse serum. TCO **2** and *trans*-cyclooctenol (TCO-OH) **10** were synthesized using a modified procedure of Fox,³¹ in which the CCO or *cis*-cyclooctenol (CCO-OH) was irradiated at 254 nm in the presence of methyl benzoate (see ESI†). For TCO-OH **10** a mixture of diastereomers (1.42 : 1) was isolated and used in preliminary studies. The major (equatorial) and minor (axial) isomers were subsequently separated for detailed kinetic analyses.

Initially the cycloaddition of **8a/8b** with TCO-OH **10** (Scheme 3) was investigated using spectrofluorometry (ex 360 nm, em 455 nm). Fluorescence of 7-hydroxycoumarin **13a** or 7-amino-4-methylcoumarin **13b** was quenched by the azido-PABC linker (probe **8a/8b**), which upon addition of TCO-OH **10** (10-fold excess) resulted in activation of **8a/8b** (Fig. 2). By 6 h 80–90% of coumarin had been released from both carbonate **8a** and carbamate **8b**. In the absence of TCO-OH **10**, a low level of carbonate hydrolysis in **8a** was observed, however, no background hydrolysis was evident for the carbamate analogue **8b**. Reaction of **8a** with CCO-OH (10-fold excess) had no effect on the release of **13a**, with only background hydrolysis measured (10% at 24 h). As amides, esters and ethers of **13a/13b** are non-fluorescent (ex 360 nm, em 455 nm),^{26,32–34} the intermediates **11b** and **12b** would not exhibit any fluorescence at the measured excitation and emission wavelengths, hence the measured fluorescence is the result of released coumarin **13a/13b**. Therefore the results from our spectrofluorometry studies imply that the reaction proceeds *via* triazoline **11b** followed by an imine intermediate such as **12b**.

To confirm that the reaction we observed in the initial spectrofluorometry studies proceeds *via* the triazoline and aldimine, and not some alternate mechanism, a series of ¹H NMR experiments in CDCl₃ and CD₃CN/D₂O were performed with **8a** (Fig. 3 and Fig. S11–S14†). Reaction of TCO-OH **10** with **8a** would have given a complex mixture of regio- and stereoisomers **11b** and **12b**, therefore, TCO **2** was used (Scheme 3, conc. **8a**: 6.7 mM, TCO **2**: 18.7 mM). This allowed us to monitor for the less complex intermediates **11a** and **12a** in the ¹H NMR spectrum. Initially we examined the reaction in CDCl₃ and observed that approx. 50% of probe **8a** had been consumed within 3 hours and converted to the triazoline **11a**. At 24 hours, trace amounts of the imine **12a** were observed, and by 5 days **12a** was clearly visible in the reaction mixture. The isomers of imine **12a** (3 : 1 ratio) were identified *via* the imine proton (N=CH) observed as two doublets at δ 7.75 (major, *J* = 5.2 Hz) and 7.77 (minor, *J* = 4.4 Hz). Interestingly, no detectable levels of the released coumarin **13a** were observed in CDCl₃, even after 5 days. This indicates that unlike the example of Shea (no triazoline detected),²⁴ our benzyloxycarbonyl triazoline **11a** and



Scheme 1 1,3-dipolar cycloaddition reported by Shea.²⁴



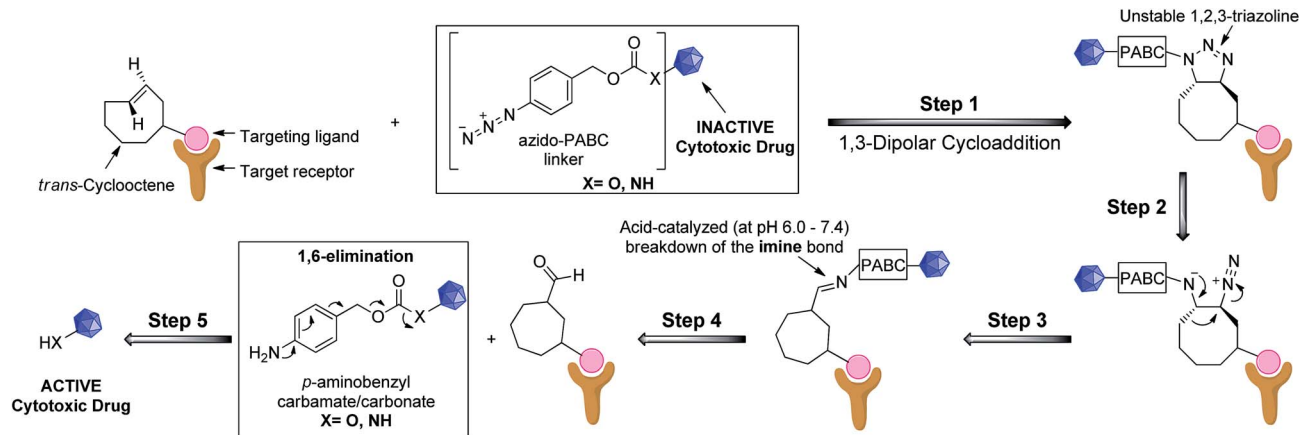
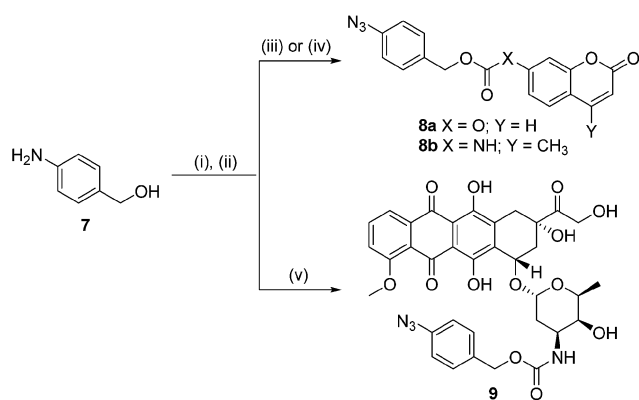
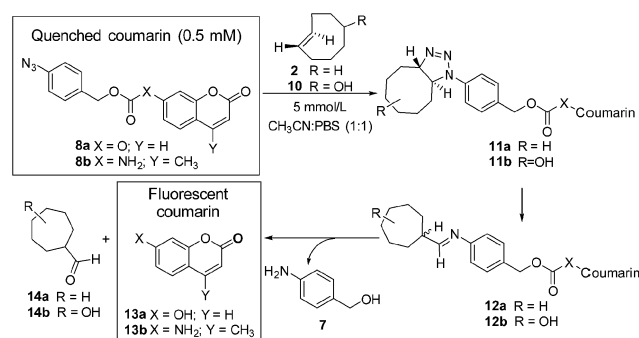


Fig. 1 Proposed general strategy for prodrug activation via a 1,3-dipolar cycloaddition. The targeting ligand could be an antibody, peptide or small molecule.



Scheme 2 Conditions: (i) NaNO_2 , 5 M HCl then NaN_3 , 0 °C, 73%; (ii) 4-nitrophenyl chloroformate, pyridine, DCM, 25 °C, 57%; (iii) 7-hydroxycoumarin, Et_3N , DMF, 25 °C, 38%; (iv) 7-amino-4-methylcoumarin, triphosgene, toluene, reflux, then 4-azidobenzyl alcohol, 25 °C, 30%; (v) doxorubicin·HCl, Et_3N , 4 Å molecular sieves, DMF, 25 °C, 69%.

imine **12a** are stable in organic solvent. If residual acid was not removed from the CDCl_3 (dependent on storage time of CDCl_3 bottle) by filtration through a short plug of basic alumina, direct conversion of probe **8a** to the coumarin **13a** occurred, with no evidence of the intermediate imine **12a** in the ^1H NMR spectrum.



Scheme 3 Model prodrug activation strategy.

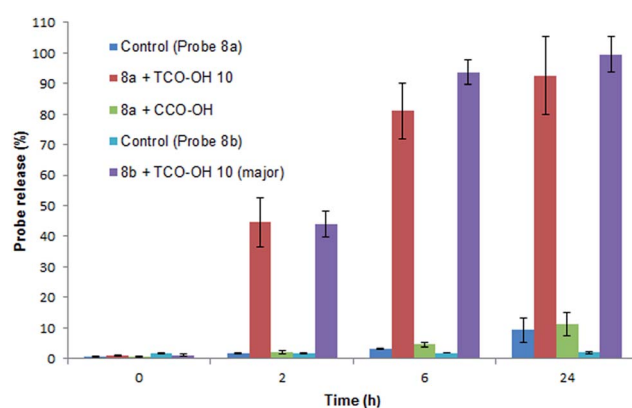


Fig. 2 Release of 7-hydroxycoumarin **13a** from **8a** and 7-amino-4-methylcoumarin **13b** from **8b** in PBS : MeCN (1 : 1), measured by fluorescence (ex 360, em 455). Error represented as $\pm\text{SD}$ ($n = 3$).

In a slightly more protic environment, $\text{CD}_3\text{CN}/\text{D}_2\text{O}$ (9 : 1), coumarin **13a** was rapidly released, with trace amounts immediately observed upon mixing (time = 0 h). At 47 hours none of the initial probe **8a** remained, and the major peaks observed were due to the release of coumarin **13a** and the imine hydrolysis product, aldehyde **14a**. In this solvent system the internal standard masked the area where the major and minor imine protons were expected, but the absence of two doublets corresponding to the aromatic protons of the imine **12a**, and the presence of the aldehyde peak at δ 9.58 (d, $J = 1.2$ Hz) indicated that the imine was rapidly hydrolyzed in the presence of water. The NMR studies indicate that water or acid is essential for protonation and conversion of the triazoline **11a/b** and imine **12a/b** intermediates to the PABC-analogue. As expected, the PABC-analogue is not observed as it undergoes a rapid 1,6-elimination to release coumarin **13a** and aldehyde **14a/b**. The ketamine and aziridine intermediates analogous to that reported for Shea's trinitrophenylazide derivatives **5** and **6** (Scheme 1)²⁴ were expected in small quantities, however, apart from possible trace amounts (see aromatic region of 6.5–7.6



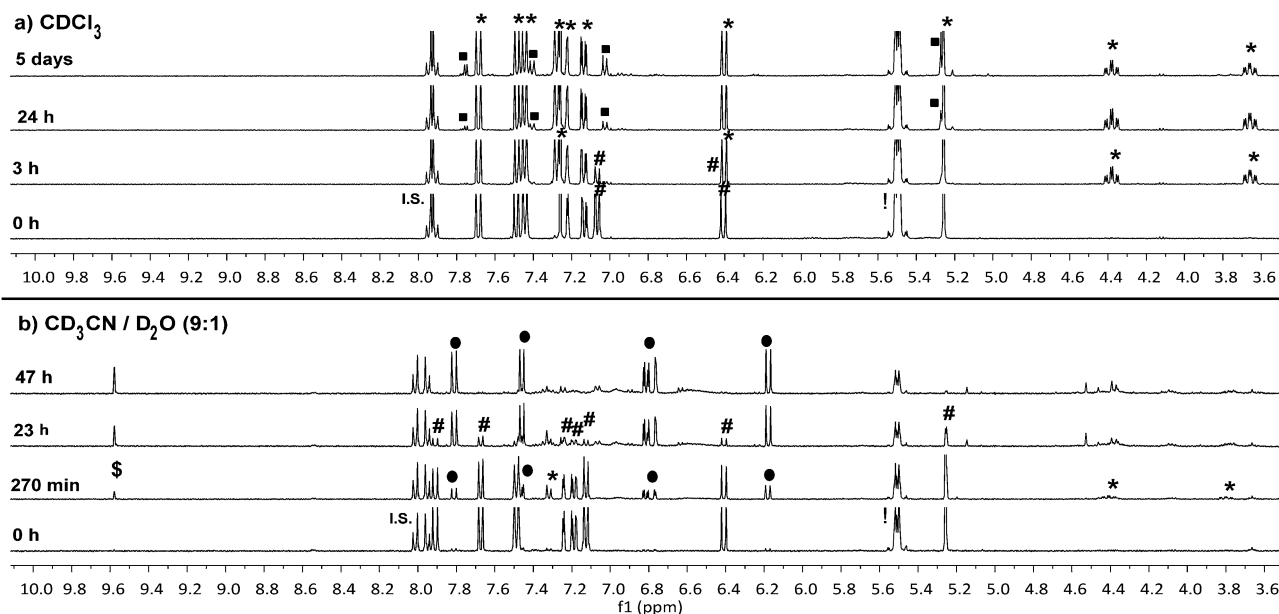


Fig. 3 ^1H NMR experiments in: (a) CDCl_3 (filtered through basic alumina) and (b) $\text{CD}_3\text{CN}/\text{D}_2\text{O}$ (9 : 1); monitoring 1,3-dipolar cycloaddition between TCO 2 and probe 8a. Legend: key structural proton shifts illustrated; #: coumarin probe 8a; *: triazoline 11a; ■: aldimine 12a; ●: 7-hydroxycoumarin 13a; \$: exocyclic aldehyde 14a; !: TCO 2; I.S.: Internal Standard, 4-iodonitrobenzene.

ppm in Fig. S14†), they were not observed in the ^1H NMR spectra. This indicates that the thermodynamically favored aldimine 12a dominates during the triazoline degradation. Based on our data from the spectrofluorometry and NMR mechanistic studies, the reaction favors the synthesis of the desired and labile aldimine ($\geq 90\%$ conversion), making it a strong candidate for orthogonal protecting group chemistry and bioorthogonal prodrug activation.

The fluorescent release and NMR studies show that TCO 2 and TCO-OH 10 activation of 8a/8b was responsible for the *in situ* generation of an aldimine with rapid release of coumarin 13a/13b in protic solvents. However, the experiments did not give an idea as to the speed for the initial 1,3-dipolar cycloaddition in protic solvents. Using RP-HPLC we were able to measure the *pseudo* first-order rate of the 1,3-dipolar cycloaddition in $\text{CH}_3\text{CN} : \text{PBS}$ (1 : 1, 37°C) *via* the disappearance of probe 8a at 254 nm and calculate the second-order rate constant (see Fig. S6 and S7†). In the presence of the TCO-OH major-10 (equatorial isomer) or minor-10 (axial isomer), the rate of the 1,3-dipolar cycloaddition was measured as $0.017 \text{ M}^{-1} \text{ s}^{-1} \pm 0.003$ and $0.027 \text{ M}^{-1} \text{ s}^{-1} \pm 0.006$, respectively. The faster rate for minor-10 can be attributed to the higher energy in the axially substituted ring,³¹ and will be important for future design of activating molecules. For comparison, the rate of the 1,3-dipolar cycloaddition between probe 8b and TCO major-10 was calculated as $0.020 \text{ M}^{-1} \text{ s}^{-1} \pm 0.0002$ ($\text{CH}_3\text{CN} : \text{PBS}$, 1 : 1), indicating that the presence of a carbamate linker does not affect the rate of cycloaddition (Fig. S8†).

Promisingly, even without modifications to the aromatic ring of the PABC linker or the TCO-OH ring, the rates are comparable to the first generation of SPAAC reactions (10^0 – $10^{-3} \text{ M}^{-1} \text{ s}^{-1}$)^{15a,15d} and are an order of magnitude faster than the

Staudinger ligation ($10^{-3} \text{ M}^{-1} \text{ s}^{-1}$).^{15a} Comparison of our reaction rates to those of Shea²⁴ demonstrate that with the highly electron-deficient tri-nitro substituted aromatic ring, a rate of $0.687 \text{ M}^{-1} \text{ s}^{-1}$ in CDCl_3 is achieved. While our rate for the cycloaddition is an order of magnitude slower than that of Shea, synthesis of optimized linkers which have been substituted with electron-withdrawing functional groups should enable us to reach or improve on these rates, particularly in an aqueous environment.

While the 1,3-dipolar cycloaddition is considered the key rate-determining step in our approach, the triazoline and imine degradation, and the final 1,6-elimination also contribute to the overall rate of drug/probe release. Therefore, our next goal was to investigate the rate of triazoline and imine degradation. Based on the spectrofluorometry results (Fig. 2) we did not expect the rates of the triazoline rearrangement and subsequent imine hydrolysis to be influenced by the nature of the *para*-substituted benzyloxy linker (carbonate *vs.* carbamate drug/probe), thus we selected the more stable carbamate probe 8b to investigate these steps (ESI Section 4†). To enable us to directly measure release of the 7-amino-4-methylcoumarin 13b from the triazoline intermediate, the 1,3-dipolar cycloaddition of 8b with TCO major-10 was monitored by ^1H NMR spectroscopy in CD_3CN and $\text{DMSO}-d_6$ (Fig. S3†). After 19 h, ^1H NMR analysis indicated that all of probe 8b had been consumed and converted to the triazoline intermediate 11b (diastereomers), with no imine, aziridine or 7-amino-4-methylcoumarin 13b observed. An aliquot of the NMR sample was then diluted (1000-fold) into PBS and the rate of triazoline and imine degradation was measured by the appearance of 13b on the spectrofluorometer (Fig. S4† ex 360, em 455). By 1 h 88% of 13b had been released, and over the first 40 min, the degradation and release



process (three steps in total) appeared to follow *pseudo* first-order kinetics with a half-life of 19 min (Fig. S5†). While we cannot delineate the rates of the three processes, the kinetics suggest that one of the steps, either triazoline degradation or imine hydrolysis is rate-limiting in a polar protic solvent. The increase in entropy and loss of CO₂ provides a significant thermodynamic driving force for the 1,6-elimination,³⁵ thus this is not expected to be rate-determining at a pH of 7.4 ($t_{1/2}$ = 17 s),²⁶ and is independent on the pK_a of the leaving group.³⁶

Our mechanistic studies with probe **8a** and **8b** demonstrate that there are likely two steps which are rate determining in our prodrug activation strategy, the 1,3-dipolar cycloaddition and either the triazoline or imine degradation. However, as we progress to *in vitro* and *in vivo* pre-targeting studies, the rates of triazoline and imine degradation become less significant. Both intermediates would be fixed to the tumor cell surface, unable to diffuse away from the tumor and exhibit off-target effects, thus demonstrating the importance for selective and rapid reactivity in the initial 1,3-dipolar cycloaddition. This will in effect determine how much drug is released at the pre-targeted tumor.

Next we examined the bioorthogonal potential of our strategy *via* the activation of our doxorubicin-based prodrug **9** with TCO-OH **10** (Scheme 4) in a model murine melanoma cell line (Table 1 and Fig. S16†). TCO-OH **10** was used in place of TCO **2**, due to its better solubility, low volatility, and potential to attach a targeting ligand in the future.

Against the melanoma cell line (Table 1 and Fig. S16†), cytotoxicity of prodrug **9** was low (IC₅₀: 49.9 μM) compared to the parent drug **15** (IC₅₀: 0.71 μM). This indicates that the azido-PABC linker deactivates **15** and is stable *in vitro*. Combining **9** with TCO-OH **10** (100 μM), itself non-toxic to cells at this concentration (Table 1 and Fig. S15†), restored activity of the prodrug *via* release of **15** (IC₅₀: 0.96 μM). CCO-OH, also non-toxic at 100 μM, had no effect on release of **15** from **9** (IC₅₀: 55.0 μM), showing that bioorthogonal activation only occurs in the presence of TCO-OH **10**. Utilizing major-**10** and minor-**10** for activation resulted in no significant difference in IC₅₀. Next we examined the cytotoxicity of **9** when activated with a more biologically relevant concentration of TCO-OH major-**10** (10 μM). To our excitement, an IC₅₀ of 4.98 μM was obtained. While the IC₅₀ is approximately 5-fold lower than activation with 100 μM TCO-OH **10**, we envisage that release of **15** at a targeted and doxorubicin-sensitive tumor (IC₅₀ in low nanomolar range) could still result in tumor cell death when prodrug **9**, or analogues thereof, are present at the tumor in the low micromolar range. From the current experiments we do not know

Table 1 IC₅₀ values for doxorubicin **15**, dox-prodrug **9**, and activation of **9** with *cis*- or *trans*-cyclooctenol **10**, incubated for 72 h at 37 °C

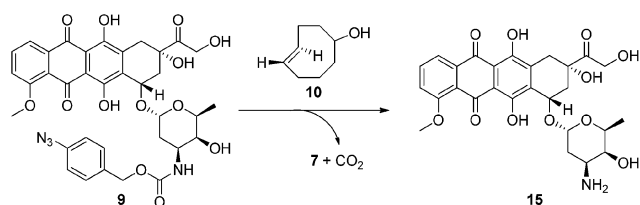
Compound	IC ₅₀ ^{a,b,c} (μM)
Doxorubicin 15	0.71 (0.66–0.77)
Dox-prodrug 9	49.9 (42.5–58.5)
9 + <i>cis</i> -cyclooctenol (100 μM)	55.0 (38.0–79.5)
9 + <i>trans</i> -cyclooctenol ^d 10 (100 μM)	0.96 (0.91–1.01)
9 + major- 10 (100 μM)	1.47 (1.36–1.60)
9 + minor- 10 (100 μM)	1.34 (1.27–1.42)
9 + major- 10 (10 μM)	4.98 (4.49–5.52)

^a IC₅₀ = concentration required to kill 50% of cells. ^b 95% confidence interval ($n \geq 6$) is shown in parenthesis. ^c Cell survival at 100 μM of CCO-OH, TCO-OH **10**, major-**10**, minor-**10** was 98%, 101%, 97% and 92%, respectively. ^d Mixture of major and minor diastereomers (1.42 : 1).

where the activation and release occurs, but suspect that it is occurring both inside and outside the cells. However, from the experiments we do know that release of **15** is promoted by the 1,3-dipolar cycloaddition, and that in our proposed *in vivo* targeting strategy (Fig. 1) release of **15** would be expected to occur outside the cell followed by diffusion of the cytotoxic drug into the closely located tumor cells.

Importantly, with only a 5-fold difference, improving the rate of the cycloaddition (*via* modifications to the aromatic ring of the azido-PABC linker^{24,37} and TCO-OH **10** ring) could lead to higher release of **15** at even lower activation concentrations of TCO-OH. Assuming one to six TCOs can be attached to each monoclonal antibody⁷ which then binds to approximately 10⁵ cell surface receptors,⁶ we estimate that a concentration of 0.4 to 2.5 μM TCO would be present on the tumor cell surface (assuming cell volume of 400 femto litre).³⁸ While prodrug **9** is significantly less toxic than the parent drug **15** (70-fold) and could be administered in relatively high doses, it will be important to improve the rate of cycloaddition for our future targeted *in vivo* studies, particularly when the number of activating TCO molecules on targeting ligands and therefore the concentration on the cell surface is limited.⁷ A faster rate for the cycloaddition will also help to overcome the relatively rapid clearance rates observed in mice ($t_{1/2}$ = minutes) for small molecules such as doxorubicin and its prodrugs,³⁹ without the requirement for larger and continuous dosing.

With proof-of-concept demonstrated *in vitro*, we next evaluated the stability and activation of prodrug **9** in mouse serum so as to determine its suitability for *in vivo* studies (ESI Section 8†). While aryl azides can be prone to thiol reduction,^{40–42} we expected this to be minimal for prodrug **9** as the most cell-relevant species (GSH and cysteine) require very high levels to carry out azide reduction.^{40,41} To confirm azide stability we examined the degradation of **9** (100 μM) in 50% mouse serum:PBS and PBS only (Table S1 and S2†). Prodrug **9** (t_R = 8.7 min) was relatively stable in mouse serum (at 37 °C), with 95%, 68%, and 56% intact at 4, 24 and 53 h, respectively (Table S1†). The amount of doxorubicin **15** (t_R = 4.2 min) released in the absence of TCO-OH **10** was also measured, and at 53 h, only 6% was observed (Table S2†), indicating that most of the prodrug **9**



Scheme 4 *In vitro* activation of prodrug **9**.



degradation was not due to azide reduction and subsequent 1,6-elimination of **15**. Activation of **9** in serum *via* the addition of TCO-OH major-**10** (500 μ M) resulted in rapid release of **15** (51% in 4 h, Table S2†). The amount of **15** which had been released following activation decreased over time (4.7% at 48 h, Table S2†), and correlated to an increase in a new peak ($t_R = 7.6$ min, Fig. S23†). The decrease in **15** and appearance of the new peak was not observed in the control (PBS only) activation experiment, with 79% of **15** observed at 48 h (Fig. S20, S24 and Table S2†), indicating that free doxorubicin is slowly metabolized in the serum or binds more strongly than prodrug **9** to serum protein. The peak at 7.6 min was very weak in the serum stability assay, confirming that the product is a metabolite of **15** and not prodrug **9**. We are also aware that TCO-OH **10** could undergo slow isomerization back to the unreactive CCO-OH, however, future *in vivo* studies will use strategically designed linkers attached to targeting ligands (*e.g.* antibodies) that are known to stabilize the strained TCO-OH *in vivo*.^{8,21}

Importantly, our serum studies are in contrast to the other potential azide prodrug activation strategy, the Staudinger ligation, in which a byproduct of the phosphine formed in the serum resulted in severely reduced reaction efficiency.³⁰ Examining the *in vivo* SPAAC reported by Bertozzi¹⁴ and Robillard⁴³ indicated that strong covalent and non-covalent interactions to serum proteins could potentially reduce the effective concentration, and therefore reactivity, of our prodrug **9** at the pre-targeted tumor. This could be detrimental to any pre-targeting strategy as the strong serum binding in the case of cyclooctyne resulted in even lower levels of *in vivo* reactivity than the sluggish Staudinger ligation.¹⁴ While both groups reported that their studied cyclooctynes (the reagent added after tumor pre-targeting) suffered from reduced *in vivo* reaction rates because of strong covalent and non-covalent interactions with serum proteins,^{14,43} the reactivity of our reagents did not appear to be hindered in the presence of the mouse serum proteins (we observed 51% of doxorubicin **15** being released in 4 h, Table S2†). The rate was slightly faster in serum:PBS than in PBS alone (34% release of doxorubicin **15** in 4 h, Table S2†), providing further evidence that *in vivo* serum protein binding of prodrug **9** should be minimized (lower binding affinity than the cyclooctynes used in SPAAC).^{14,43} Promisingly, the second order rate of 1,3-dipolar cycloaddition for prodrug **9** (0.1 mM) with TCO major-**10** (10 mM) measured under *pseudo* first-order reaction conditions in 50% serum:PBS (Fig. S25†) was calculated to be $0.137 \pm 0.012 \text{ M}^{-1} \text{ s}^{-1}$. This is an order of magnitude faster than that observed for the model probes **8a** and **8b** in an acetonitrile : PBS mixture (1 : 1), and two orders of magnitude faster than the Staudinger ligation, demonstrating that we can expect faster 1,3-dipolar cycloadditions under increasingly aqueous conditions.⁴⁴

Conclusions

To the best of our knowledge there are no examples of *in vivo* click reactions for chemically triggered release of drugs, making our work reported here and that of Robillard^{14,45} all the more significant. Although challenges await as we progress to *in vivo*

pre-targeting studies, we have demonstrated, for the first time, a strain promoted 1,3-dipolar cycloaddition with potential use in prodrug activation, imaging applications and orthogonal protecting group strategies. The reaction proceeds with a second-order rate equivalent to the first generation SPAAC and is 1–2 orders of magnitude faster than the Staudinger reaction enabling rapid orthogonal deprotection of azido-PABC protected amino and hydroxyl groups under mild conditions. While azido-PABC carbonate-linked drugs are unlikely to be stable in a biological milieu, the potential of azido-PABC carbamate drugs for bioorthogonal prodrug activation is demonstrated in a melanoma cell line, with the model doxorubicin prodrug **9** remaining deactivated until reaction with TCO-OH **10**, upon which it regains the cytotoxicity of the parent drug **15**. The prodrug also demonstrates good stability in mouse serum over biologically relevant circulation times for cytotoxic drugs (minutes to hours) and due to the rapid reactivity observed in serum:PBS, the azido-prodrug **9** does not appear to bind strongly to, or react with, serum proteins like the cyclooctynes and triphenylphosphines of the *in vivo* SPAAC and Staudinger ligation pre-targeting studies.^{14,30,43}

We are currently investigating ways to improve the activation rate of our prodrugs for future *in vivo* studies with modifications to the PABC linkers and TCO molecules (*e.g.* electron-withdrawing functionalities such as nitro²⁴ and fluorine groups³⁷). Additionally, we are examining other linkers with azide triggers that can be used as stable alternatives to the carbonate linker, expanding the scope of our activation strategy to both alcoholic and phenolic drugs.

Acknowledgements

This research was funded in part by a University of Otago Research Grant (UORG) and a contract from the Health Research Council (HRC) of New Zealand (A.B.G.). The authors would also like to thank Sarah Katzemich for her contributions to the synthesis of the 7-hydroxycoumarin probe.

Notes and references

- 1 J. R. Trounce, *Br. J. Clin. Pharmacol.*, 1979, **8**, 205–207.
- 2 I. Collins and P. Workman, *Nat. Chem. Biol.*, 2006, **2**, 689–700.
- 3 R. Mahato, W. Tai and K. Cheng, *Adv. Drug Delivery Rev.*, 2011, **63**, 659–670.
- 4 J. Rautio, H. Kumpulainen, T. Heimbach, R. Oliyai, D. Oh, T. Jarvinen and J. Savolainen, *Nat. Rev. Drug Discovery*, 2008, **7**, 255–270.
- 5 A. Warnecke, *Drug Delivery in Oncology: From Basic Research to Cancer Therapy*, ed. F. Kratz, P. Senter and H. Steinhagen, Wiley-VCH, Weinheim, Germany, 1st edn, 2011, pp. 553–589.
- 6 R. V. J. Chari, M. L. Miller and W. C. Widdison, *Angew. Chem., Int. Ed.*, 2014, **53**, 3796–3827.
- 7 N. K. Devaraj, R. Upadhyay, J. B. Haun, S. A. Hilderbrand and R. Weissleder, *Angew. Chem., Int. Ed.*, 2009, **48**, 7013–7016.



- 8 R. Rossin, S. M. J. van Duijnhoven, T. Lappchen, S. M. van den Bosch and M. S. Robillard, *Mol. Pharmaceutics*, 2014, **11**, 3090–3096.
- 9 K. D. Bagshawe, *Drug Delivery in Oncology: From Basic Research to Cancer Therapy*, ed. F. Kratz, P. Senter and H. Steinhagen, Wiley-VCH, Weinheim, Germany, 1st edn, 2011, pp. 169–186.
- 10 K.-C. Chen, S.-Y. Wu, Y.-L. Leu, Z. M. Prijovich, B.-M. Chen, H.-E. Wang, T.-L. Cheng and S. R. Roffler, *Bioconjugate Chem.*, 2011, **22**, 938–948.
- 11 R. M. Versteegen, R. Rossin, W. ten Hoeve, H. M. Janssen and M. S. Robillard, *Angew. Chem., Int. Ed.*, 2013, **52**, 14112–14116.
- 12 E. M. Sletten and C. R. Bertozzi, *Acc. Chem. Res.*, 2011, **44**, 666–676.
- 13 N. K. Devaraj, R. Upadhyay, J. B. Haun, S. A. Hilderbrand and R. Weissleder, *Angew. Chem., Int. Ed.*, 2009, **48**, 7013–7016.
- 14 P. V. Chang, J. A. Prescher, E. M. Sletten, J. M. Baskin, I. A. Miller, N. J. Agard, A. Lo and C. R. Bertozzi, *Proc. Natl. Acad. Sci. U. S. A.*, 2010, **107**, 1821–1826.
- 15 For selected reviews on bioorthogonal chemistry see: (a) E. M. Sletten and C. R. Bertozzi, *Angew. Chem., Int. Ed.*, 2009, **48**, 6974–6998; (b) N. K. Devaraj and R. Weissleder, *Acc. Chem. Res.*, 2011, **44**, 816–827; (c) M. F. Debets, S. S. van Berkel, J. Dommerholt, J. Dirks, F. P. J. T. Rutjies and F. L. van Delft, *Acc. Chem. Res.*, 2011, **44**, 805–815; (d) C. P. Ramil and Q. Lin, *Chem. Commun.*, 2013, **49**, 11007–11022; (e) M. King and A. Wagner, *Bioconjugate Chem.*, 2014, **25**, 825–839; (f) A. Borrmann and J. C. M. van Hest, *Chem. Sci.*, 2014, **5**, 2123–2134; (g) D. M. Patterson, L. A. Nazarova and J. A. Prescher, *ACS Chem. Biol.*, 2014, **9**, 592–605.
- 16 M. Azoulay, G. Tuffin, W. Sallem and J.-C. Florent, *Bioorg. Med. Chem. Lett.*, 2006, **16**, 3147–3149.
- 17 R. van Brakel, R. C. M. Vulders, R. J. Bokdam, H. Grull and M. S. Robillard, *Bioconjugate Chem.*, 2008, **19**, 714–718.
- 18 K. Gorska, A. Manicardi, S. Barluenga and N. Wissinger, *Chem. Commun.*, 2011, **47**, 4364–4366.
- 19 J. T. Weiss, J. C. Dawson, K. G. Macleod, W. Rybski, C. Fraser, C. Torres-Sanchez, E. E. Patton, M. Bradley, N. O. Carragher and A. Unciti-Broceta, *Nat. Commun.*, 2014, **5**, 3277.
- 20 J. T. Weiss, J. C. Dawson, C. Fraser, W. Rybski, C. Torres-Sanchez, M. Bradley, E. E. Patton, N. O. Carragher and A. Unciti-Broceta, *J. Med. Chem.*, 2014, **57**, 5395–5404.
- 21 R. Rossin, S. M. van den Bosch, W. ten Hoeve, M. Carvelli, R. M. Versteegen, J. Lub and M. S. Robillard, *Bioconjugate Chem.*, 2013, **24**, 1210–1217.
- 22 M. R. Karver, R. Weissleder and S. A. Hilderbrand, *Angew. Chem., Int. Ed.*, 2012, **51**, 920–922.
- 23 R. H. Smith Jr, B. D. Wladkowski, J. E. Taylor, E. J. Thompson, B. Pruski, J. R. Klose, A. W. Andrews and C. J. Michejda, *J. Org. Chem.*, 1993, **58**, 2097–2103.
- 24 K. J. Shea and J.-S. Kim, *J. Am. Chem. Soc.*, 1992, **114**, 4846–4855.
- 25 P. L. Carl, P. K. Chakravarty and J. A. Katzenellenbogen, *J. Med. Chem.*, 1981, **24**, 479–480.
- 26 I. A. Muller, F. Kratz, M. Jung and A. Warnecke, *Tetrahedron Lett.*, 2010, **51**, 4371–4374.
- 27 R. A. Gatenby and R. J. Gillies, *Nat. Rev. Cancer*, 2004, **4**, 891–899.
- 28 D. Neri and C. T. Supuran, *Nat. Rev. Drug Discovery*, 2011, **10**, 767–777.
- 29 A. S. Bailey and J. E. White, *J. Chem. Soc. B*, 1966, 819–822.
- 30 D. J. Vugts, A. Vervoort, M. Stigter-van Walsum, G. W. M. Visser, M. S. Robillard, R. M. Versteegen, R. C. M. Vulders, J. D. M. Herscheid and G. A. M. S. van Dongen, *Bioconjugate Chem.*, 2011, **22**, 2072–2081.
- 31 M. Royzen, G. P. A. Yap and J. M. Fox, *J. Am. Chem. Soc.*, 2008, **130**, 3760–3761.
- 32 J.-P. Goddard and J.-L. Reymond, *Curr. Opin. Biotechnol.*, 2004, **15**, 314–322.
- 33 Y. Meyer, J.-A. Richard, M. Massonneau, P.-Y. Renard and A. Romieu, *Org. Lett.*, 2008, **10**, 1517–1520.
- 34 W. Gao, B. Xing, R. Y. Tsien and J. Rao, *J. Am. Chem. Soc.*, 2003, **125**, 11146–11147.
- 35 H. Y. Lee, X. Jiang and D. Lee, *Org. Lett.*, 2009, **11**, 2065–2068.
- 36 B. M. Sykes, M. P. Hay, D. Bohinc-Herceg, N. A. Helsby, C. J. O'Connor and W. A. Denny, *J. Chem. Soc., Perkin Trans. 1*, 2000, 1601–1608.
- 37 F. Schoenebeck, D. H. Ess, G. O. Jones and K. N. Houk, *J. Am. Chem. Soc.*, 2009, **131**, 8121–8133.
- 38 E. H. Chapman, A. S. Kurec and F. R. Davey, *J. Clin. Pathol.*, 1981, **34**, 1083–1090.
- 39 H. P. Svensson, V. M. Vruthula, J. E. Emswiler, J. F. MacMaster, W. L. Cosand, P. D. Senter and P. M. Wallace, *Cancer Res.*, 1995, **55**, 2357–2365.
- 40 J. V. Staros, H. Bayley, D. N. Strandring and J. R. Knowles, *Biochem. Biophys. Res. Commun.*, 1978, **80**, 568–572.
- 41 S. Chen, Z. Chen, W. Ren and A. Ai, *J. Am. Chem. Soc.*, 2012, **134**, 9589–9592.
- 42 P. K. Sasmal, S. Carregal-Romero, A. A. Han, C. N. Streu, Z. Lin, K. Namikawa, S. L. Elliot, R. W. Koster, W. J. Parak and E. Meggers, *ChemBioChem*, 2012, **13**, 1116–1120.
- 43 S. M. van den Bosch, R. Rossin, P. Renart Verkerk, W. ten Hoeve, H. M. Janssen, J. Lub and M. S. Robillard, *Nucl. Med. Biol.*, 2013, **40**, 415–423.
- 44 J. W. Wijnen, R. A. Steiner and J. B. F. N. Engberts, *Tetrahedron Lett.*, 1995, **36**, 5389–5392.
- 45 R. Rossin and M. S. Robillard, *Curr. Opin. Chem. Biol.*, 2014, **21**, 161–169.

